

Supporting Information

Ultrastretchable, High-performance, and Crosstalk-free Proximity and Pressure Bimodal Sensor Based on Ionic Hydrogel Fibers for Human-Machine Interfaces

*Haojun Ding, Zixuan Wu, Hao Wang, Zijing Zhou, Yaoming Wei, Kai Tao, Xi Xie and Jin Wu**

H. Ding, Z. Wu, H. Wang, Z. Zhou, Y. Wei, Prof. X. Xie and Prof. J. Wu

State Key Laboratory of Optoelectronic Materials and Technologies and the Guangdong Province Key Laboratory of Display Material and Technology, School of Electronics and Information Technology, Sun Yat-sen University, Guangzhou 510275, China

E-mail: wujin8@mail.sysu.edu.cn

Prof. K. Tao

Ministry of Education Key Laboratory of Micro and Nano Systems for Aerospace, Northwestern Polytechnical University, Xi'an 710072, China

The PDF file includes:

- **Figure S1.** Weight losses of the pristine hydrogel fiber and the 50wt% LiBr percolated hydrogel fiber at 25°C and 46% RH.
- **Figure S2.** Schematic illustrating the cross-sectional profile of the hydrogel fiber-based bimodal sensor.
- **Figure S3.** Structure and performance of the original bimodal sensor prepared with an elastomer film cover, which failed to differentiate proximity and pressure.
- **Figure S4.** Capacitance response induced by moving the conductor for 1cm at different initial positions.

- **Figure S5.** Magnified image of Figure 3e from 72.5 to 75.0 s.
- **Figure S6.** The capacitance change of the sensor in response to exhaling is negligible.
- **Figure S7.** The resistance variation responding to an approaching finger at different distances.
- **Figure S8.** Homemade tensile machine for measuring proximity and pressure responses of the sensor under stretching states.
- **Figure S9.** The change of the initial capacitance of the sensor with tensile strain.
- **Table S1.** Comparison of the performance of state-of-the-art capacitive proximity/pressure bimodal sensors.

Other Supplementary Material for this manuscript includes the following:

- **Movie S1.** Video showing capacitance change of the sensor to different numbers of fingers.
- **Movie S2.** Video manifesting capacitance change of the sensor to different gestures.
- **Movie S3.** Video showing capacitance change of the sensor to the vertical movement of palm at different speeds above the sensor.
- **Movie S4.** Video showing capacitance change of the sensor to the approach of a human hand to the sensor at different moving speeds.
- **Movie S5.** Video depicting the response of the sensor attached on the screen to different finger pressure.
- **Movie S6.** Video showing the resilience of the bimodal sensor to punctures and impacts.

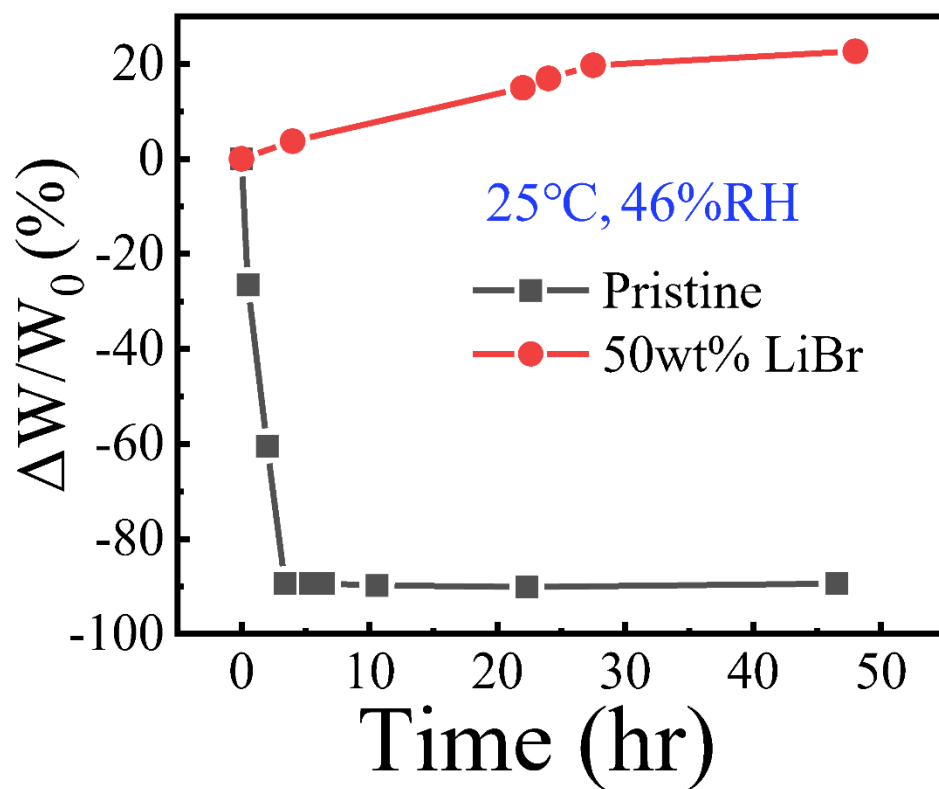


Figure S1. Weight losses of the pristine hydrogel fiber and the 50wt% LiBr percolated hydrogel fiber at 25°C and 46% RH.

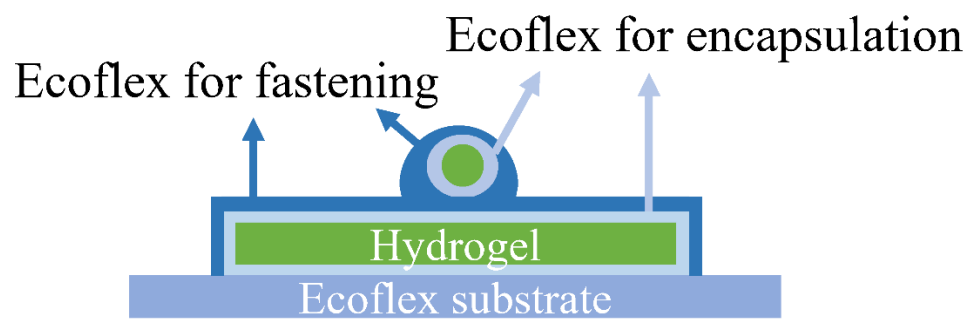


Figure S2. Schematic illustrating the cross-sectional profile of the hydrogel fiber-based bimodal sensor.

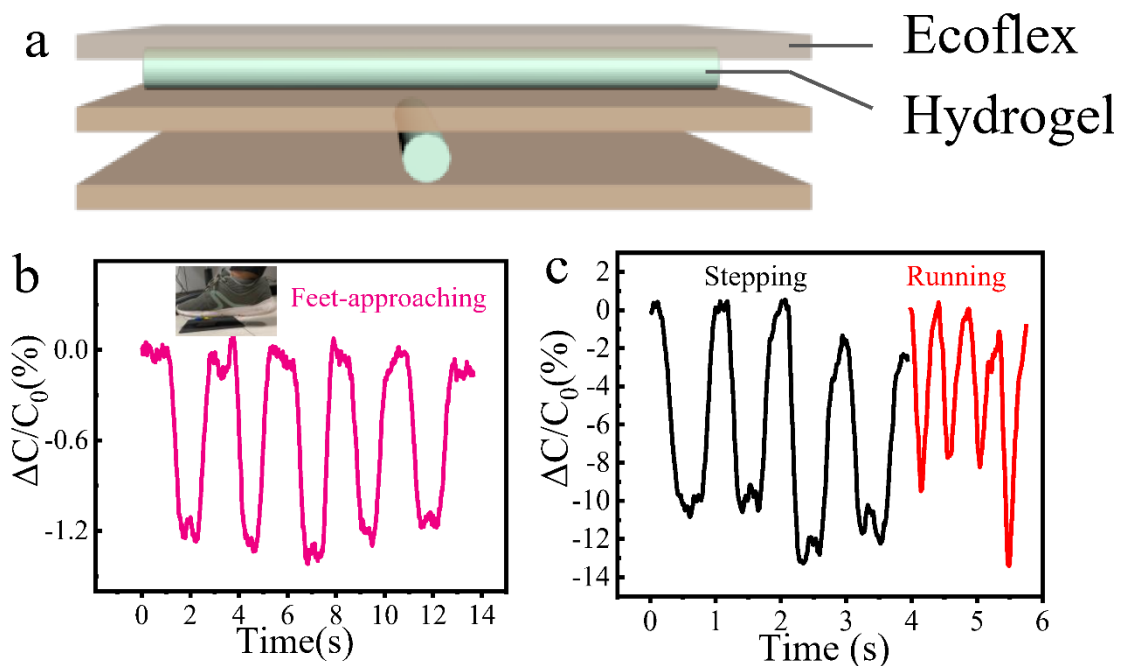


Figure S3. Structure and performance of the original bimodal sensor prepared with an elastomer film cover, which failed to differentiate the proximity and pressure. a) Scheme illustrating the sensor structure obtained by using an elastomer to sandwich two fibers and another elastomer film for covering the fibers. b) Response of the original sensor to the repeated approaching of the feet of a volunteer. c) Response of the original sensor to repeated stepping or running of a 60-kilogram man on the sensor.

To explore the effect of the elastomer structure on the sensing performance, a hydrogel fiber with silver wires tied at both ends was placed on the Ecoflex film and covered with a thin layer of Ecoflex prepolymer. Then, another identical fiber was placed orthogonally over the original fiber. Finally, the superficial fiber was covered with the Ecoflex prepolymer again, followed by the coverage of another Ecoflex film to obtain the original bimodal hydrogel fiber sensor. Sensors made in this way are tough enough

to allow a 60kg-person to stand or even run on them. However, due to the thick Ecoflex film, the pressure response of the sensor is small and far less than the proximity response, and the capacitance will still decrease during compression, thus failing to achieve accurate pressure detection. Therefore, the preparation process was optimized on this basis. By dipping the hydrogel fibers into the Ecoflex prepolymer to form a thin Ecoflex coating layer, the pressure sensitivity can be effectively increased, allowing the sensor's capacitance to rise when subjected to pressure, thus achieving accurate pressure detection.

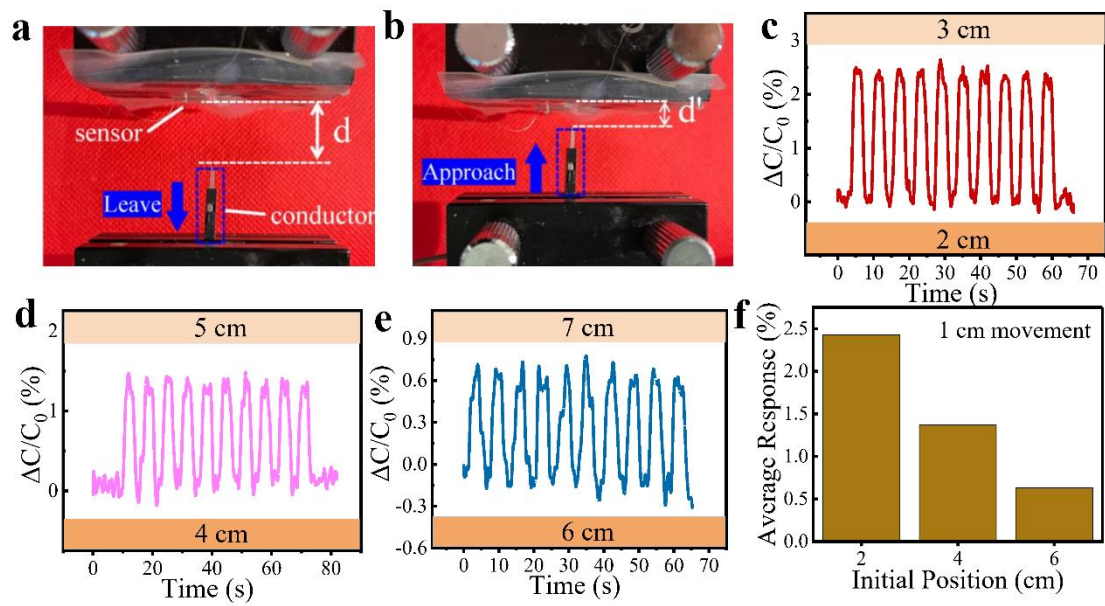


Figure S4. Capacitance response induced by moving the conductor for 1 cm at different initial positions. a-b) Photos of using the conductor to simulate the hand to leave and approach the sensor. c-e) Capacitance response induced by moving the conductor for 1 cm at different initial positions. f) Average capacitance response of the sensor extracted from c-e.

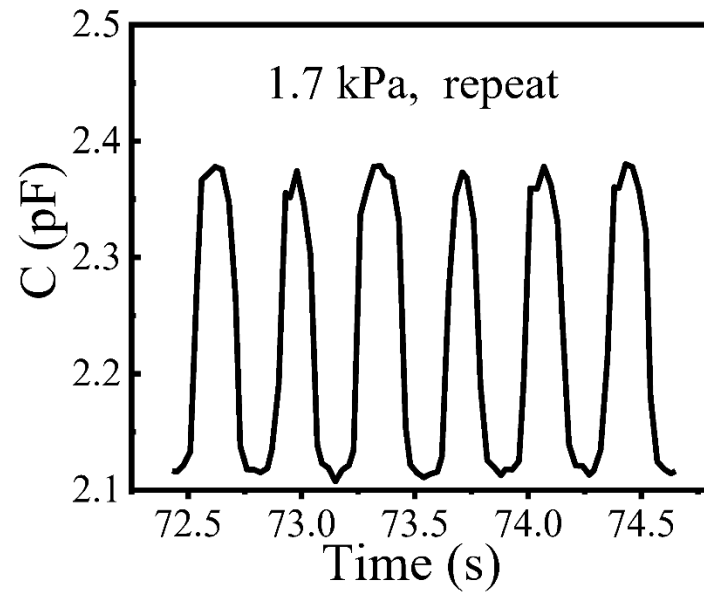


Figure S5. Magnified image of Figure 3e from 72.5 to 75.0 s.

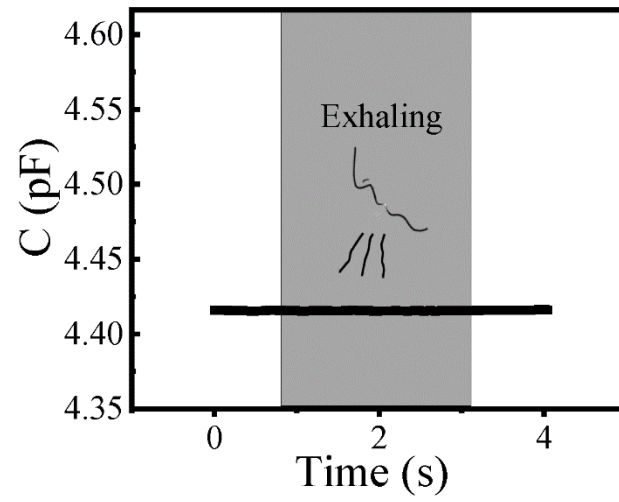


Figure S6. The capacitance change of the sensor in response to exhaling is negligible, showing good immunity to humidity.

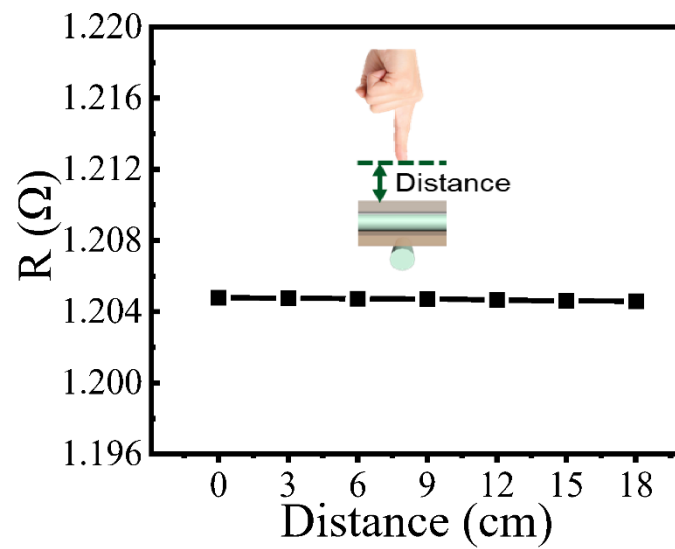


Figure S7. The resistance variation responding to an approaching finger at different distances is extremely small.

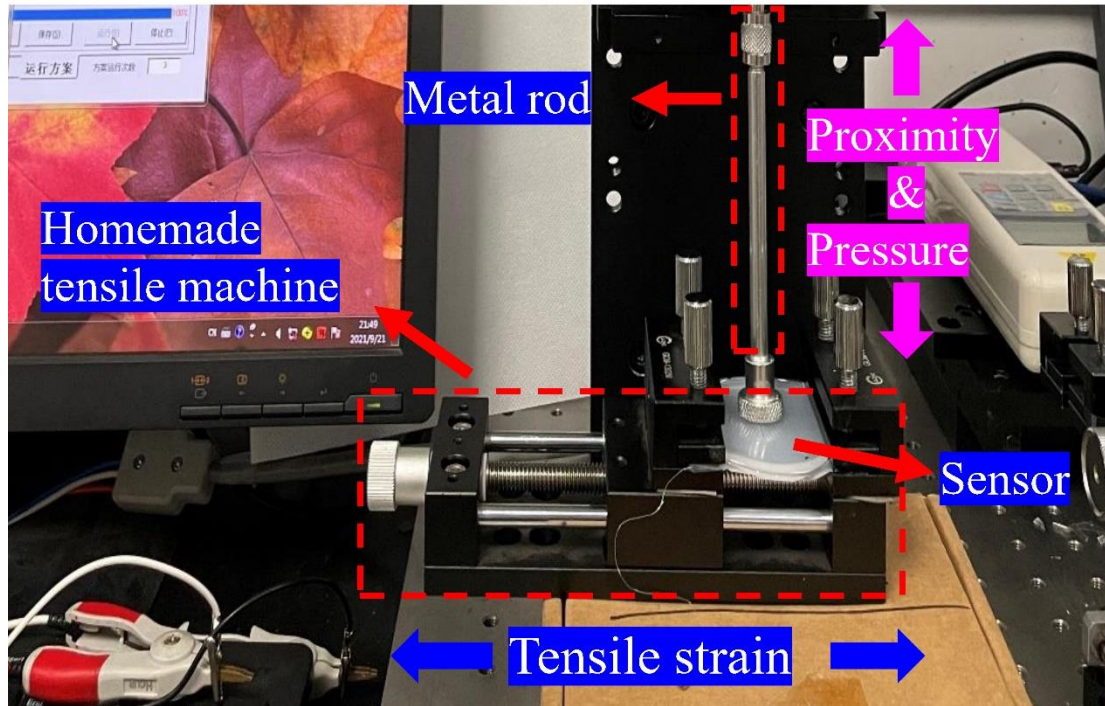


Figure S8. Homemade tensile machine for measuring proximity and pressure responses of the sensor under different stretching states.

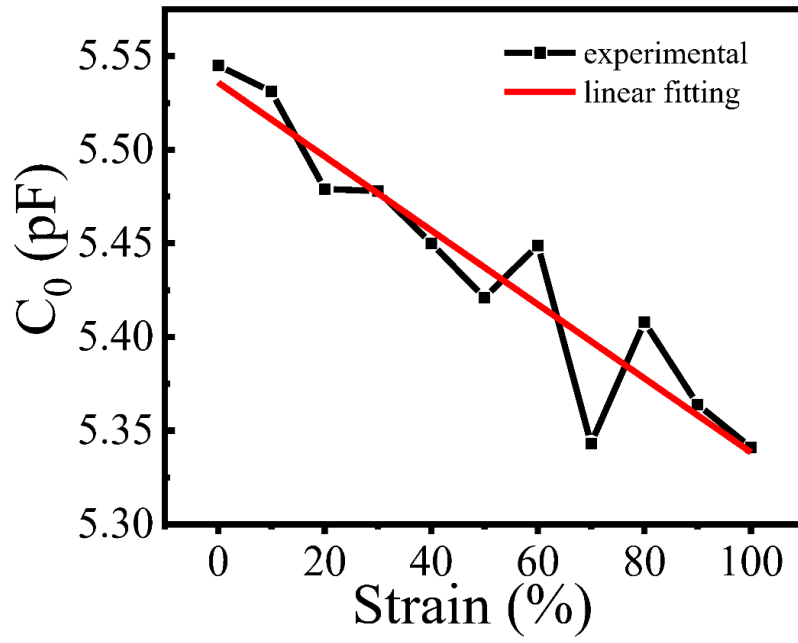


Figure S9. The change of the initial capacitance of the sensor with tensile strain.

Table S1. Comparison of the performance of state-of-the-art capacitive proximity/pressure bimodal sensors based on different transducing materials.

Sensing Materials	Pressure						Proximity				Refs.
	Trans	Strain (%)	Sens (kPa ⁻¹)	t _{Res} (ms)	t _{Rec} (ms)	LOD (Pa)	Sens (cm ⁻¹)	Range (cm)	t _{Res} (ms)	t _{Rec} (ms)	
PAM/Alg-Ca	Yes	100	0.91	40	40	63	3.17%	18	90	90	This work
P:P/SWCNT	Yes	40	0.1	82	82	0.6	/	30	/	/	1
MWCNTs	No	/	0.86	5	/	10	/	/	/	/	2
AgNW	Yes	/	0.20	/	/	29	/	9	/	/	3
PMMA/PI	No	/	0.02	/	/	7.3	/	4	/	/	4
AiFoam	No	/	0.378	33	19	/	/	12	24	24	5

Alg-Ca, calcium alginate; P:P, poly(3,4-ethylenedioxythiophene):poly(styrenesulfonate); SWCNT, single-walled carbon nanotube; MWCNTs, multiwalled carbon nanotubes; AgNW, silver nanowire; PMMA/PI, poly (methyl methacrylate)/polyimide; AiFoam, artificially innervated foam; Trans, transparency; Strain, maximum tensile strain in working state. Sens, sensitivity; t_{Res}/t_{Rec}, response time/recovery time; LOD, limit of detection.

References

1. P. Zhao, R. Zhang, Y. Tong, X. Zhao, T. Zhang, Q. Tang and Y. Liu, *ACS Appl. Mater. Interfaces*, 2020, **12**, 55083-55093.
2. J. O. Kim, S. Y. Kwon, Y. Kim, H. B. Choi, J. C. Yang, J. Oh, H. S. Lee, J. Y. Sim, S. Ryu and S. Park, *ACS Appl. Mater. Interfaces*, 2019, **11**, 1503-1511.
3. M. R. Kulkarni, R. A. John, M. Rajput, N. Tiwari, N. Yantara, A. C. Nguyen and N. Mathews, *ACS Appl. Mater. Interfaces*, 2017, **9**, 15015-15021.
4. Q. Hua, J. Sun, H. Liu, R. Bao, R. Yu, J. Zhai, C. Pan and Z. L. Wang, *Nat. Commun.*, 2018, **9**, 244.
5. H. Guo, Y. J. Tan, G. Chen, Z. Wang, G. J. Susanto, H. H. See, Z. Yang, Z. W. Lim, L. Yang and B. C. K. Tee, *Nat. Commun.*, 2020, **11**, 5747.